

## Analysis of three dimensional equivalent static wind loads of symmetric high-rise buildings based on wind tunnel tests

Shuguo Liang<sup>1</sup>, Lianghao Zou<sup>\*1</sup>, Dahai Wang<sup>2</sup> and Guoqing Huang<sup>3</sup>

<sup>1</sup>*School of Civil and Building Engineering, Wuhan University, 8 South Donghu Road, Wuhan, China*

<sup>2</sup>*School of Civil Engineering and Architecture, Wuhan University of Technology, 122 Luoshi Road, Wuhan, China*

<sup>3</sup>*School of Civil Engineering, Southwest Jiaotong University, 111 Beiyiduan, Erhuanlu, Chengdu, China*

(Received November 28, 2013, Revised August 27, 2014, Accepted August 31, 2014)

**Abstract.** Using synchronous surface pressures from the wind tunnel test, the three dimensional wind load models of high-rise buildings are established. Furthermore, the internal force responses of symmetric high-rise buildings in along-wind, across-wind and torsional directions are evaluated based on mode acceleration method, which expresses the restoring force as the summation of quasi-static force and inertia force components. Accordingly the calculation methods of equivalent static wind loads, in which the contributions of the higher modes can be considered, of symmetric high-rise buildings in along-wind, across-wind and torsional directions are deduced based on internal forces equivalence. Finally the equivalent static wind loads of an actual symmetric high-rise building are obtained by this method, and compared with the along-wind equivalent static wind loads obtained by China National Standard.

**Keywords:** high-rise building; equivalent static wind load; mode acceleration method; internal force responses

### 1. Introduction

Wind loads on high-rise buildings are three-dimensional (Solari 1985, Liang *et al.* 2002 and 2004), including along-wind and across-wind forces, as well as the torque. Therefore, wind-induced structural responses shall be three-dimensional as well and the combined action under wind loads in these three directions must be considered in the structural design. The current research on the equivalent static wind loads (ESWLs) of high-rise buildings is mainly focused on the along-wind direction. In 1960s, Davenport (1967) proposed the along-wind ESWL evaluation method: Gust Loading Factor (GLF). This sparked various improvements on the determination of ESWLs for high-rise buildings. Due to the distinct features of the background and resonant responses, it is more convenient and physically meaningful to model the background and resonant ESWLs (BESWL and RESWL) separately, especially when the background response is noticeable. BESWL can be modeled by Load Response Correlation (LRC) (Kasperski and Niemann 1992). The RESWL is obtained by distributing the wind-induced inertial force (WIF) over the building

---

\*Corresponding author, Associate professor, E-mail: [liangsgwhu@sohu.com](mailto:liangsgwhu@sohu.com)

height (Davenport 1985), which is adopted in Chinese codes (Zhang 1988). Although the equivalence of GLF and WIF is achieved for the displacement response of the fundamental mode, there are significant differences between their load distributions for other responses. Zhou *et al.* (1999, 2000) proposed the model of ESWL composed of background component by LRC method and resonance component by WIF method. Ke *et al.* (2012) investigated the coupling effects between resonance modes and coupled term between background and resonant components, and proposed a new methodology which can take their contribution to ESWLs into consideration for cooling tower structures. Huang and Chen (2007) studied wind load effect and ESWL of high-rise buildings using measured pressure data from wind tunnel tests and analyzed the contributions of the high order modes to the structural responses. Wang and Liang (2010) established the ESWL model of high-rise buildings in along-wind direction based on the internal force equivalent principle. Blaise and Denoel (2013) extended the concept of LRC method to the displacement-response correlation (DRC) method, which covers the background and resonant contributions of the concerned responses, and established principal static wind loads. These studies have shown that there are significant differences on the distribution of ESWL along the building height and there is a need to develop an improved ESWL evaluation method.

For the across-wind and torsional directions, Recommendations for Loads on Buildings by Architecture Institute of Japan (AIJ 1996) recommends the calculation methods for ESWL and wind induced vibration response in these two directions of high-rise buildings. Chen and Kareem (2004) presented a new model for evaluating the ESWL on tall buildings with uncoupled responses in along-wind, across-wind and torsional directions. Nevertheless, this model only considers the contribution of the fundamental structural mode in each direction. Quan and Gu (2012) also proposed the ESWL model in across-wind direction of super high-rise buildings, which is composed of background component calculated by LRC method and resonance components calculated by WIF method. Recently, Kwon and Kareem (2013) compared the major international wind codes and standards on tall buildings, and investigated survivability and serviceability of the buildings in both of along-wind and across-wind directions.

Along with the universal application of multi-point scanning surface pressures on rigid models in wind tunnel tests, there is an urgent need to develop an improved ESWL evaluation method with considerations of the three-dimensional wind-induced responses for high-rise buildings with the height of more than 200 m. As the high-rise buildings have become higher and slender, their natural frequencies of the lower-order vibration modes become smaller, and the contributions of the second-order or even high-order vibration modes to the wind-induced dynamic responses cannot be neglected. As the buildings have symmetric shapes and mass centers coincident with resistance centers, the structure exhibits one-dimensional mode shapes, and wind-induced dynamic responses and the ESWL on each directions can be analyzed individually (AIJ 1996, Chen and Kareem 2004). However, once the eccentricity of the mass center with respect to rigidity center and geometry center on some floors of high-rise buildings is large, for example, if the preceding eccentricity reaches more than 10% of the width of the cross section, the mode shape shall be three dimensional and noticeable coupling effects shall occur among the wind-induced vibrations in three directions. In this situation, the contributions of three-dimensional coupling effects among along-wind, across-wind and torsional directions should be considered in wind-induced dynamic responses and the ESWL (Islam 1992, Chen and Kareem 2005, Huang *et al.* 2009, Chan *et al.* 2010, Huang *et al.* 2011, Spence *et al.* 2011, Rosa *et al.* 2012). Based on the pressure integration technique, a recent procedure developed by Aly (2013a) can predict wind-induced lateral-torsional coupled responses accurately for high-rise buildings with complex mode shapes and non-uniform

mass distribution, and the calculation results showed a good agreement with recent design standards.

Based on the mode acceleration method, this paper deduces the calculation method of internal force for the floors of symmetrical high-rise buildings under the actions of the three-dimensional wind loads, and proves that the statistical correlation of the three-dimensional fluctuating wind loads does not make contributions to these internal force in each direction. The calculation method of ESWLs in along-wind, across-wind and torsional directions, which can consider the contributions of high-order modes, is proposed based on the above-mentioned work. An engineering example shows that this method and its results are valuable reference for the wind-resistant design of super high-rise buildings.

## 2. Calculation of equivalent wind load by mode acceleration method

### 2.1 Calculation of internal force response

Based on the theories of structural dynamics, the structural internal force response under the actions of the dynamic loads can be regarded as the results of restoring or elastic force. Then when the wind acts along a main horizontal axis of high-rise buildings, and the coupling of the three-dimensional vibration does not occur (coincidence of structure mass center and rigidity center), the vibration equation of the wind induced dynamic response in along-wind, across-wind and torsional directions of high-rise buildings can be expressed by the inter-floor model as follows

$$\{F\} = [K]\{Y\} = \{P\} - [M]\{\ddot{Y}\} - [C]\{\dot{Y}\} \tag{1}$$

in which,  $\{F\}$  is the restoring force or restoring moment vector in a principal horizontal or torsional direction;  $\{Y\}$  is the structural displacement or rotation vector;  $\{P\}$  is the random wind load vector in along-wind, across-wind and torsional directions;  $[M]\{\ddot{Y}\}$  is the inertia force or inertial moment on each floor and  $[M]$  is structure mass or moment of inertia matrix;  $[C]\{\dot{Y}\}$  is the damping force (or moment) on each floor and  $[C]$  is the damping matrix..

Thus, the solution of horizontal displacement and rotation can be approximately evaluated by

$$\{\tilde{y}(t)\} = [K]^{-1}\{P\} - [K]^{-1}[C]\sum_{i=1}^J \dot{q}_i(t)\{\varphi\}_i - [K]^{-1}[M]\sum_{i=1}^J \ddot{q}_i(t)\{\varphi\}_i \tag{2}$$

in which,  $\{\tilde{y}(t)\}$  is the structural horizontal displacement or rotation vector after the approximation;  $J$  is mode number under which the dynamic effect is significant;  $q_i(t)$  is the generalized coordinate of vibration mode  $i$ ;  $\{\varphi\}_i$  is the mode shape of the  $i$ th mode.;  $\omega_i$  is the natural circular frequency of vibration mode  $i$  and  $\{\varphi\}_i$  is the mode shape of the  $i$ th mode. As the damping of the high-rise building is rather small, the damping term can be neglected. Note  $[K]^{-1}[M]\{\varphi\}_i = \{\varphi\}_i / \omega_i^2$ , then Eq. (2) can be approximately rewritten as

$$\{\tilde{y}(t)\} = [K]^{-1}\{P\} - \sum_{i=1}^J \frac{1}{\omega_i^2} \ddot{q}_i(t)\{\varphi\}_i \tag{3}$$

The first term on the right side of the equation is the quasi-static portion of the displacement, and is the displacement response when the fluctuating wind loads have not been dynamically

amplified by the structure system, thus the quasi-static displacement is only related to  $\{P(t)\}$  at the same time. As the natural frequency of the high-rise building structure generally changes quickly with the increase of mode order,  $1/\omega_i^2$  in the second term on the right side of the equation improves the astringency. Eq. (3) is well known as the mode acceleration method, which essentially corresponds to the analysis of separating the dynamic responses into the background and resonant components. The elastic force or moment response can also be obtained as follows

$$\{\tilde{f}(t)\} = \{P\} - [M] \sum_{i=1}^J \ddot{q}_i(t) \{\varphi\}_i \tag{4}$$

where  $\{f_B(t)\} = \{P(t)\}$  can be regarded as quasi-static term;  $\{f_I(t)\} = [M] \sum_{i=1}^J \ddot{q}_i(t) \{\varphi\}_i$  can be regarded as inertia force term. Then Eq. (4) can be rewritten as

$$\{\tilde{f}(t)\} = \{f_B(t)\} - \{f_I(t)\} \tag{5}$$

When the contribution of the multiple order modes is considered, the obtained elastic force (moment) response of the multi-degree-of-freedom system can be expressed as

$$\{\tilde{f}(t)\} = \{P\} - \ddot{q}_1(t)[M]\{\varphi\}_1 - \dots - \ddot{q}_J(t)[M]\{\varphi\}_J \tag{6}$$

Based on Eq. (6), the covariance matrix of  $\{\tilde{f}\}$  can be obtained as

$$[\sigma_f^2] = E\left[\{\tilde{f}\}\{\tilde{f}\}^T\right] \tag{7}$$

As the natural frequencies of high-rise buildings are separated, the correlation between the accelerations of two modes can be omitted, and analysis related to this result can be accomplished in light of the formula proposed by Gu and Zhou (2009). Meanwhile, the correlation between the fluctuating wind load and the acceleration response for each mode is also rather small and can be neglected (Wang and Liang 2010). Then the covariance matrix  $[\sigma_f^2]$  of structural elastic force (moment) can be expressed as follows

$$\begin{aligned} \sigma_f^2 = \sigma_B^2 + \sigma_I^2 = & \begin{bmatrix} \sigma_{B11}^2 & \sigma_{B12}^2 & \dots & \sigma_{B1N}^2 \\ \sigma_{B21}^2 & \sigma_{B22}^2 & \dots & \sigma_{B2N}^2 \\ \dots & \dots & \dots & \dots \\ \sigma_{BN1}^2 & \dots & \dots & \sigma_{BNN}^2 \end{bmatrix} \\ + \sigma_{y1}^2 & \begin{bmatrix} M_1^2 \phi_{11}^2 & M_1 M_2 \phi_{11} \phi_{12} & \dots & M_1 M_N \phi_{11} \phi_{1N} \\ M_1 M_2 \phi_{12} \phi_{11} & M_2^2 \phi_{12}^2 & \dots & M_2 M_N \phi_{12} \phi_{1N} \\ \dots & \dots & \dots & \dots \\ M_1 M_N \phi_{1N} \phi_{11} & \dots & \dots & M_N^2 \phi_{1N}^2 \end{bmatrix} \\ + \dots + \sigma_{yj}^2 & \begin{bmatrix} M_1^2 \phi_{j1}^2 & M_1 M_2 \phi_{j1} \phi_{j2} & \dots & M_1 M_N \phi_{j1} \phi_{jN} \\ M_2 M_1 \phi_{j2} \phi_{j1} & M_2^2 \phi_{j2}^2 & \dots & M_2 M_N \phi_{j2} \phi_{jN} \\ \dots & \dots & \dots & \dots \\ M_N M_1 \phi_{jN} \phi_{j1} & \dots & \dots & M_N^2 \phi_{jN}^2 \end{bmatrix} \end{aligned} \tag{8}$$

In the above equation,  $\sigma_B^2$  is the covariance matrix of the wind load in along-wind, across-wind and torsional directions respectively, which is the first term on the right side of the above equation;  $\sigma_I^2$  is the covariance matrix of the structural inertia force, and corresponds to the summation of the terms from the second term to the last term on the right side of the above equation.

Without a loss of generality, for the linear high-rise structural system, any internal force response  $r_n$  at floor  $n$  is linearly related to elastic force (moment) on the mass (the moment of inertia) of floor  $m$ . Based on the random vibration theory, the variance of any internal force responses of floor  $n$  of high-rise buildings is as follows

$$\sigma_{r_n}^2 = \sum_{m=n}^N \sum_{k=n}^N \sigma_f^2(m,k) s_m s_k \tag{9}$$

where  $N$  is the total number of floors.  $\sigma_f^2(m,k)$  is the covariance of the elastic forces (moments)  $f_m$  and  $f_k$  on floors  $m$  and  $k$  of the structure respectively; and  $s_m$  and  $s_k$  are the response functions to express the internal force response of floor  $n$  caused by unit force (moment of couple) on floors  $m$  and  $k$ . For the internal force responses concerned in the design, for example, the variance of the shear force or torque on floor  $n$  can be expressed as follows

$$\sigma_{V_n}^2 = \sum_{m=n}^N \sum_{k=n}^N \sigma_f^2(m,k) \tag{10}$$

The variance of bending moment on floor  $n$  can be expressed in the same manner as

$$\sigma_{M_n}^2 = \sum_{m=n}^N \sum_{k=n}^N \sigma_f^2(m,k) (z_m - z_n)(z_k - z_n) \tag{11}$$

in which,  $z_m$ ,  $z_n$  and  $z_k$  are the heights of floors  $m$ ,  $n$  and  $k$  respectively.

### 2.2 Statistical correlation of 3-D wind loads

It can be proved that when the coupling of three-dimensional vibration of high-rise buildings does not occur, the statistical correlation among three-dimensional wind loads of high-rise buildings, i.e., wind loads of high-rise buildings in along-wind, across-wind and torsional directions, does not make contributions to the internal force between the floors.

According to the structural random vibration theories,  $R(z_n, t)$ , the internal force response of a high-rise building at floor  $n$  induced by the dynamic wind loads, can be expressed as follows

$$R(z_n, t) = \sum_{i=1}^J A_i(z_n) q_i(t) \tag{12}$$

in which,  $A_i(z_n)$  is the internal force response function of mode  $i$ ;  $q_i(t)$  is the generalized coordinate function of mode  $i$ ;  $J$  is the number of vibration mode.  $A_i(z_n)$  can be obtained by the following equation

$$A_i(z_n) = \sum_{k=1}^{3N} M_k \omega_i^2 \phi_{ik} I(k, n) \quad (13)$$

where  $3N$  is the number of the dimensions of mode shape vector, and  $N$  is the number of the building floor;  $I(k, n)$  is the influence function of the unit load, and represents the internal force at floor  $n$  caused by the unit load at the floor of the  $k$ -th element of mode shape vector, and acting along the same direction of the  $k$ -th element.  $M_k$  is the mass or moment of inertia of floor  $k$ . After  $A_i(z_n)$  is obtained, the following equation can be used to calculate the mean square of internal force  $R(z_n, t)$

$$\sigma_R^2(z_n) = \sum_{i=1}^J \sum_{j=1}^J A_i(z_n) A_j(z_n) \int_0^\infty H_i(i\omega) H_j(-i\omega) S_{ij}^*(\omega) d\omega \quad (14)$$

where  $H_i(i\omega)$  is the complex frequency response function of mode  $i$ ;  $S_{ij}^*(\omega) = \frac{\Phi_i^T \mathbf{S}_P(\omega) \Phi_j}{M_i^* M_j^*}$  is

the cross spectral density function of mode  $i$  and  $j$ .  $M_j^* = \Phi_j^T \mathbf{M} \Phi_j$  is the generalized mass of mode  $j$ .  $\Phi_j$  is  $3N$  dimensional mode shape vector. When the coupling does not occur for the structural three-dimensional vibration,  $2N$  values of the mode shape in the two directions where vibration does not take place become zero.

$\mathbf{S}_P(\omega) = \begin{bmatrix} \mathbf{S}_{uu}(\omega) & \mathbf{S}_{uv}(\omega) & \mathbf{S}_{ut}(\omega) \\ \mathbf{S}_{vu}(\omega) & \mathbf{S}_{vv}(\omega) & \mathbf{S}_{vt}(\omega) \\ \mathbf{S}_{tu}(\omega) & \mathbf{S}_{tv}(\omega) & \mathbf{S}_{tt}(\omega) \end{bmatrix}$  is the spectral density matrix of the structural

three-dimensional wind load. If the floor number of the high-rise building is  $N$  and the three-dimensional coupling vibration is considered, the vibration mode number of a multi-degree-of-freedom system for the floor model of high-rise buildings shall be  $M=3N$ . Due to the statistical correlation of three-dimensional fluctuating wind load of high-rise building, all sub-matrixes or part of the sub-matrixes located at the non-main diagonal in the three-dimensional wind load spectral density matrix are not zero generally. Then, whether the coupling of mode shapes in the three directions occurs or not, the covariance of displacement response of modes  $i$  and  $j$  is not zero generally, i.e., the integral in Eq. (14) is not zero. However, in the case of the internal force response function, Eq. (14) will be different. Observing the internal force response function of mode  $i$ , i.e., Eq. (13), if Eq. (14) is used to calculate a horizontal principal axial internal force (shear or bending moment), both  $A_i(z_n)$  and  $A_j(z_n)$  are not zero when the three-dimensional mode shape is coupled. When the mass center, rigidity center of the structure and aerodynamic center (i.e., geometry center) are coincident each other, mode shapes in every directions are not mutually coupled. The mode shape function degenerates from  $3N$  dimensional vector into  $N$  dimensional vector ( $N$  is the number of floors). If  $\Phi_i$  is the translational mode shape in the same direction with the horizontal axial internal force obtained in Eq. (14) and  $\Phi_j$  is the torsional mode shape,  $A_i(z_n)$  is not zero obviously and  $A_j(z_n)$  must be zero. As the  $I(k, n)$  in the expression of  $A_j(z_n)$ , represents the required horizontal principal axial internal force at the floor  $n$  caused by the unit torque (horizontal moment of couple) on any floor  $k$ , which is obviously zero.

From this we can conclude that when the mass center, rigidity center and geometry center of each floor of high-rise buildings are in coincidence, the statistical correlation of three-dimensional fluctuating wind loads of high-rise buildings does not make contributions to the internal force between floors in all directions, i.e. only the internal force contributions of background component induced by fluctuating wind loads and the corresponding resonance component induced by inertial forces in the same direction should be considered.

### 2.3 Calculation of internal force equivalent wind load

The following equation can be used to calculate the internal force equivalent wind loads of high-rise buildings in the two horizontal principal axial and torsional directions under all wind azimuths

$$P_E(z) = \overline{P(z)} + \mu \sqrt{P_B^2(z) + P_I^2(z)} \tag{15}$$

in which,  $\overline{P(z)}$  is the average wind load. When wind approaches along the horizontal principal axial direction of the symmetrical structure, the mean wind loads in the across-wind direction and torsional direction are zero. Otherwise, the mean wind loads will be not zero on all three directions. Clearly, the mean component can be easily incorporated in the final ESWL.  $P_B(z)$  is the equivalent wind load of background component, which can also be called quasi-static equivalent wind load;  $P_I(z)$  is the equivalent wind load of the inertia force (moment) component;  $\mu$  is the peak factor. Eq. (15) can be deduced from the methodology proposed by Holmes (2002).

The following equation can be used to calculate the internal force response variance of floor  $k$  caused by the background component

$$\sigma_{R_B}^2(z_n) = \sum_{m=n}^N \sum_{k=n}^N \int_0^\infty S_p(m, k, \omega) d\omega s_m s_k \tag{16}$$

In the equation,  $N$  is the number of the floors.  $S_p(m, k, \omega)$  is a horizontal principal axial (or torsional) wind load cross spectrum of floor  $m$  and floor  $k$ . Considering equivalence of internal force, the RMS of internal force response at floor  $n$  caused by the background component should be equal to internal force caused by the background component equivalent wind load

$$\sigma_{R_B}(z_n) = \sum_{k=n}^N P_B(z_k) s_k \tag{17}$$

in which,  $P_B(z_k)$  is the background component equivalent wind load of floor  $k$ . Through the simultaneousness of the above two equations, the background component equivalent wind load of each floor can be obtained.

The following equation can be used to calculate the internal force response variance of floor  $n$  caused by inertia force (moment)

$$\begin{aligned} \sigma_{R_I}^2(z_n) = & \sigma_{y1}^2 \left[ \sum_{k=n}^N M_k \phi_{1k} s_k \right]^2 + \sigma_{y2}^2 \left[ \sum_{k=n}^N M_k \phi_{2k} s_k \right]^2 + \dots \\ & + \sigma_{yj}^2 \left[ \sum_{k=n}^N M_k \phi_{jk} s_k \right]^2 \end{aligned} \tag{18}$$

in which,  $\sigma_{yi}^2$  is the acceleration response variance of mode  $i$ . Considering equivalence of internal force, the RMS of internal force response at floor  $n$  caused by the inertia force (moment) should be equal to internal force caused by the inertia force (moment) equivalent wind load:

$$\sigma_{R_i}(z_n) = \sum_{n=k}^N P_1(z_k) s_k \quad (19)$$

where  $P_1(z_k)$  is the inertial force (moment) component equivalent wind load of floor  $k$ . Based on Eqs. (18) and (19), the inertial force (moment) component equivalent wind load of each floor can be obtained. It should be noted that the mass of each floor in the above equations shall be changed into moment of inertia of each floor to the central vertical axis, and the linear displacement, linear velocity and linear acceleration along the main horizontal axis shall be changed into angular displacement, angular velocity and angular acceleration if the torque is to be calculated.

Suppose the high-rise building is symmetrical, its mass center, rigidity center and geometrical center are in coincidence, and each floor slab of the building is rigid. The high-rise buildings can be simplified into a multi-degree-of-freedom system with each floor center as the mass center. According to the frequency domain method of random vibration theories, the acceleration response variance of mode  $i$  in the two principal horizontal axial and torsional directions of high-rise buildings can be expressed as follows

$$\sigma_{ki}^2 = \int_0^{\infty} S_{ki}(\omega) d\omega \quad k=x, y, \theta \quad (20)$$

in which,  $S_{ki}(\omega)$  is the spectrum density function of mode  $i$  of  $k$  axial acceleration (or angular acceleration), and can be expressed as

$$S_{ki}(\omega) = \frac{\omega^4 |H_i(i\omega)|^2 S_{p_i}^*(\omega)}{M_i^{*2}} \quad (21)$$

where  $H_i(i\omega)$  is the complex frequency response function of mode  $i$  in each axial direction of the structure.  $M_i^* = \Phi_i^T \mathbf{M} \Phi_i$  is the generalized mass of mode  $i$  in each axial direction of the structure,  $S_{p_i}^*(\omega) = \Phi_i^T \mathbf{S}_p(\omega) \Phi_i$  is the generalized load spectrum density function of mode  $i$  in each axial direction of the structure, where  $\mathbf{M}$  and  $\mathbf{S}_p(\omega)$  are mass (or moment of inertia) matrix and load spectral density matrix in each axial direction of the structure respectively;  $\Phi_i$  is the  $i$ th mode shape in each axial direction.

### 3. Example and analysis

An actual project of a super high-rise building to be built is taken as an example to study the structural three dimensional internal force equivalent wind loads by the method presented in this paper. The super high-rise building is 250 m in height, the main building is a rectangle chamfer cross-section construction, and the maximal width and depth of the cross-section are 53.85 m and 45.05 m, respectively. This high-rise building is located in the flow field formed by the complex

building groups, thus, the wind tunnel test must be carried out to determine the wind loads of the structure.

### 3.1 Wind tunnel test

This test is carried out in HD-2 wind tunnel laboratory of Hunan University. The wind tunnel aerodynamic contour is 53 m long, 18 m wide, and it is a duplex testing section boundary layer wind tunnel. This test is carried out in the first test section. The length of this test section is 17 m, the cross section of model test area is 3m wide and 2.5 m high, and the wind speed of the test section is 1 ~ 58 m/s, which is adjustable continuously. The diameter of its working turntable is 1.8 m. Fig. 1 shows the test model in wind tunnel. It adopts spires and cubic elements in front of the test model to simulate the atmospheric boundary layer wind field. According to the local actual terrain, Class C landform defined in China's code is used to simulate the wind field. The geometry scale ratios of the wind field and the model are 1:200, and the main buildings within 300 m surrounding this structure are simultaneously simulated. The wind profile, turbulence intensity and turbulence integral scale  $L_t^x$  of this simulated wind field are shown in Figs. 2-4 respectively. The simulated wind speed spectrum is in good agreement with the Von Karman spectrum, which is shown in Fig. 5.



Fig. 1 Model in wind tunnel

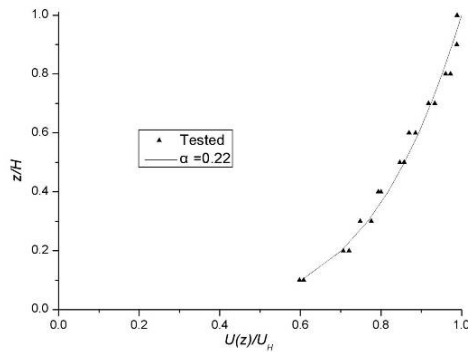


Fig. 2 Average wind speed profile

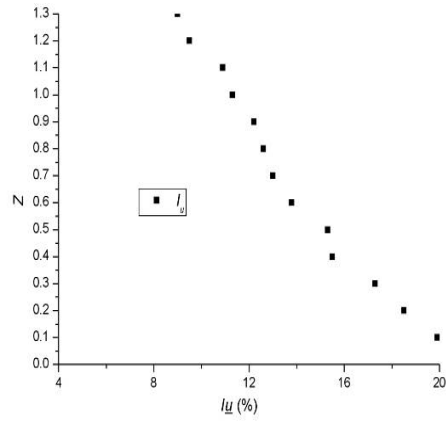


Fig. 3 Turbulence Intensity profile

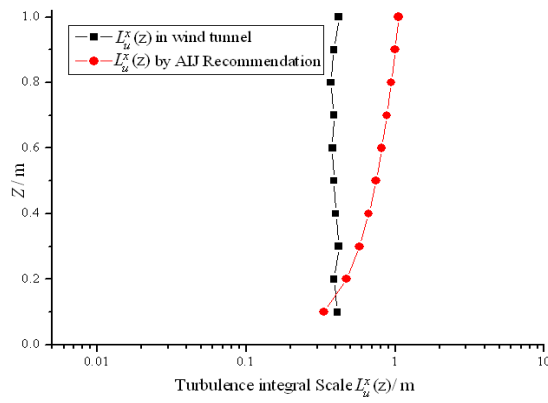


Fig. 4 Turbulence intergrale scale

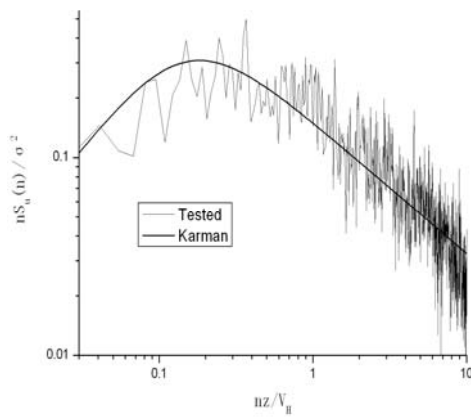


Fig. 5 Normalized wind speed spectrum

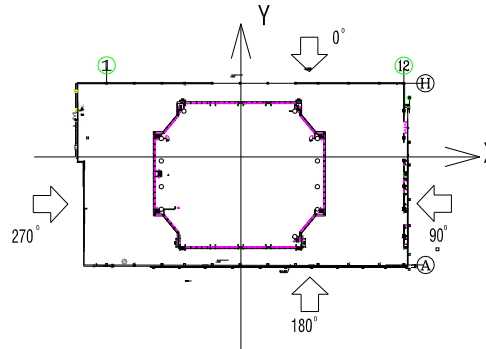


Fig. 6 Testing wind azimuths

The cobra anemometer of Probe 100 series produced by Australia TFI Company is installed at 1.0 m high in the left front of the model to measure the reference wind speed of wind tunnel tests. In order to measure the time histories of wind pressure throughout the model, total 498 pressure transducers are distributed on the model surface, and the DTC net electronic pressure scanning valve system made by American PSI Scanning Valve Company is used to measure the model surface pressure. Eight scanning valves are used to scan the pressure signals of all measurement points. The sampling time of fluctuating pressure is 20s, the sampling frequency of each measuring point is 330 Hz, and the test wind speed is approximately 10.8 m/s. By rotating working turntable to simulate wind azimuths from 0 ° to 360°, we have 24 testing wind azimuths with angle interval 15 ° in the test, as shown in Fig. 6.

### 3.2 Calculation and analysis of internal force equivalent wind load

After obtaining the time history of wind pressure on the building model surface from the wind tunnel test, the time histories of 3-D layer wind forces of the building model can be acquired by properly integrating simultaneous wind pressures on the pressure taps at the same layer weighted by their tributary areas, and this approach was recently refined by Aly (2013b). Furthermore, the time history of structural three-dimensional wind loads and three-dimensional wind load spectra can be acquired. Combining with the structural dynamic parameters obtained from the finite element model of the structure, the internal force equivalent wind loads of the building are calculated by using the method introduced in this paper. The natural frequencies and damping ratios for the 1<sup>st</sup> and 2<sup>nd</sup> modes of the structure in X-axial, Y-axial and torsional directions are given in Table 1, and the 1<sup>st</sup> and 2<sup>nd</sup> mode shapes of the structures in X-axial, Y-axial and torsional directions are illustrated in Fig. 7 respectively.

Table 1 The frequencies and damping ratios of the 1<sup>st</sup> and 2<sup>nd</sup> modes in each direction

	X-axial direction		Y-axial direction		Torsional direction	
	1st	2nd	1st	2nd	1st	2nd
Frequency/Hz	0.232	0.723	0.184	0.641	0.305	0.851
Damping ratios	0.022	0.023	0.022	0.023	0.014	0.016

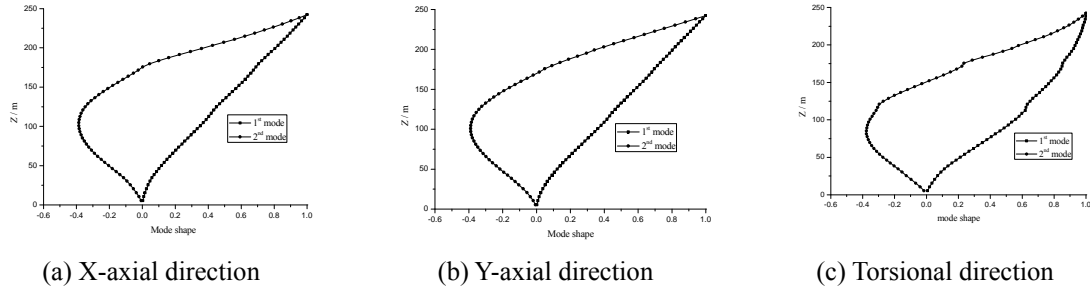


Fig. 7 The mode shapes of the structure

Fig. 8 shows the contribution to the structural acceleration from each vibration mode along X axis and Y axis under  $0^\circ$  wind azimuth (i.e., the wind is perpendicular to X axis, and the long side is windward). It can be seen from Fig. 8, in the case of  $0^\circ$  wind azimuth, when considering the contribution of the second-mode of the structure, the RMS acceleration responses along X axis (across-wind direction) and Y axis (along-wind direction) at the top of the structure increase by 5.0% and 15.7% respectively. In case of  $90^\circ$  wind azimuth, (i.e., the wind is perpendicular to Y axis, and the short side is windward), the contributions of the second mode of the structure along X axis and Y axis at the top of the structure are 18.6% and 1.8% respectively. Obviously, ignoring the contribution of the second mode would underestimate wind-induced vibration responses of the structure to a rather great extent. Similarly, during the calculation of structural equivalent wind loads of inertia force term, the obtained results will be inclined to danger if the contribution of the second vibration mode is neglected.

In order to study the characteristics of structural equivalent wind loads in case of  $0^\circ$  and  $90^\circ$  wind azimuths, each layer shearing force and bending moment equivalent wind loads along X axis and Y axis of the building and each layer torsional equivalent wind load are analyzed. Fig. 9 is the comparison diagram between the quasi-static force term equivalent wind loads and inertia force term equivalent wind loads along X axis and Y axis under  $0^\circ$  wind azimuth; Fig. 10 is the comparison diagram between the quasi-static force term equivalent wind loads and inertia force term equivalent wind loads in torsional direction under  $0^\circ$  wind azimuth; Fig. 11 is the deviation between the shearing force equivalent wind loads and bending moment equivalent wind loads under  $0^\circ$  wind azimuth.

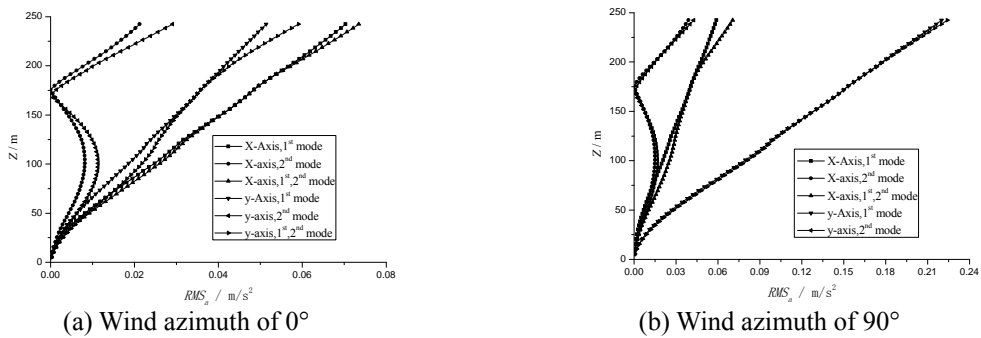


Fig. 8 RMS acceleration responses along X axis and Y axis

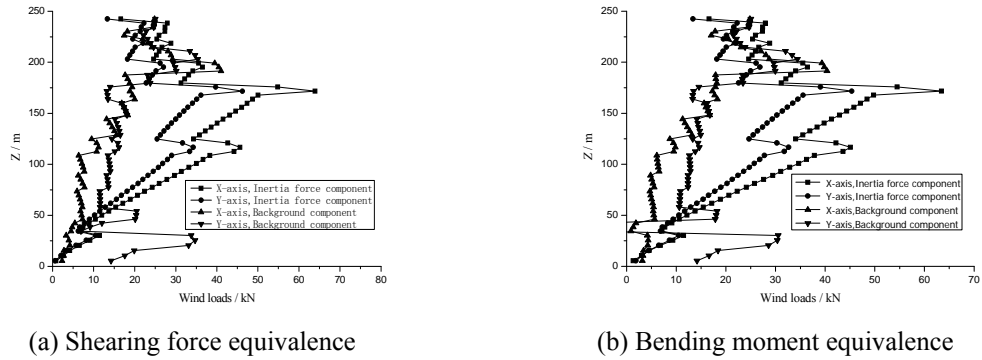


Fig. 9 Comparison of inertia force term and quasi-static force term equivalent wind loads along X axis and Y axis under 0°wind azimuth

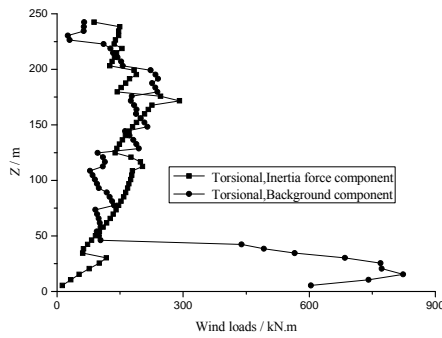


Fig. 10 Comparison of inertia force term and quasi-static force term equivalent wind loads in torsional direction under 0°wind azimuth

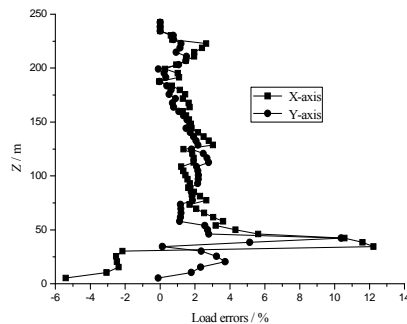


Fig. 11 Deviation between the shearing force and bending moment equivalent wind loads under 0°wind azimuth

It can be observed from Figs. 9 and 10, that the inertia force term of equivalent wind loads is slightly larger than the quasi-static force term of equivalent wind loads, but in the same order of magnitude. While carrying out the structural wind resistant design, only considering the contribution of the inertia force term and ignoring that of the quasi-static force term to structure will greatly underestimate the wind loads of the structure. As Fig. 11 shows, the difference between shearing force equivalent wind loads and bending moment equivalent wind loads is smaller, and the error is generally less than 5%; when carrying out the structural wind resistant design, either of these internal forces equivalent wind loads can be adopted.

The structural ESWLs distributed along the height of the building are shown as Figs. 12-14.

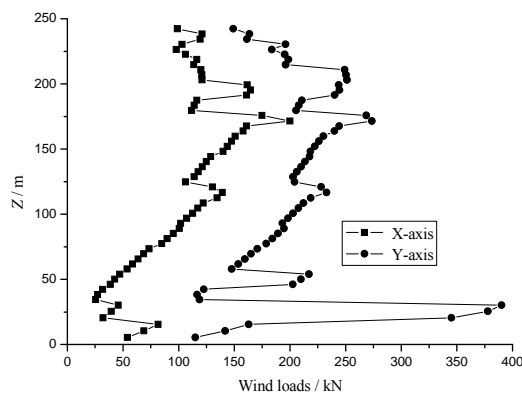


Fig. 12 ESWLs along X axis and Y axis under  $0^\circ$  wind azimuth

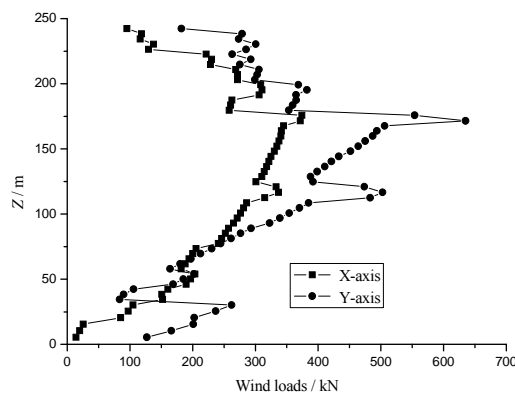


Fig. 13 ESWLs along X axis and Y axis under  $90^\circ$  wind azimuth

It can be observed from Figs. 12-14, when wind direction is perpendicular to the horizontal principal axis, the ESWLs of the building in along-wind, across-wind and torsional directions, all of these three loads cannot be neglected. When wind flow acts perpendicular to X axis (the long side is windward), its ESWLs in along-wind direction is larger than the ESWLs in cross-wind direction, and when wind flow acts perpendicular to Y axis (short side is windward), the magnitudes of the ESWLs in along-wind and in across-wind directions differ from each other slightly. When wind direction is perpendicular to Y axis (the short side is windward), the ESWLs in torsional direction is larger than those when wind direction is perpendicular to X axis (the long side is windward).

In order to investigate the ESWLs acquired by the method proposed by this paper and those by China's national code(GB50009-2012), as well as those provided by existing methods, the comparison of distribution of the ESWLs in along-wind direction along the height of the building obtained by the method of this paper and those obtained by China's national code, as well as those obtained by the method of Chen and Kareem (2004), when wind flow acts along 0° and 90° wind azimuths respectively, are shown in Fig. 15.

It can be seen from Fig. 15, for both wind azimuth of 0° and 90°, ESWLs in along-wind direction obtained by Chen and Kareem are the largest, and they are much great than those obtained by China's code, and also rather larger than, as well as a little bit larger than, those obtained by the method of this paper in wind azimuth of 0° as well as 90°, respectively. Meanwhile, the ESWLs in along-wind direction along the height of the building by the method of this paper are fairly larger than those by China National Standard no matter wind azimuth is 0° or 90°. Because the calculated average wind loads, i.e., the first term in the right side of Eq. (15), are the same for both China's code and the method of this paper, the calculated dynamic components of ESWLs, i.e., the second term in the right side of Eq. (15), by China's code as well as by the method of this paper considering the contributions of the first mode and the first two modes respectively, are illustrated in Fig. 16 to compare the differences among them. Fig. 16 shows that the main contribution for the deviation between ESWLs obtained by China's code and the method of this paper is due to the larger dynamic components obtained by the method of this paper only considering the first mode, and the contribution of the second mode by the method of this paper is minor. Further analysis indicates, the equivalent wind load of background component as well as inertia force component considering the contribution of the first mode by the method of this paper are fairly larger than those by China's code respectively.

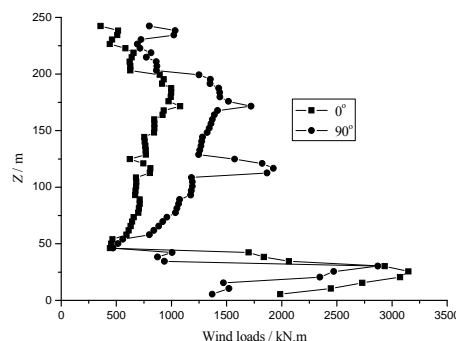


Fig. 14 ESWLs in torsional direction

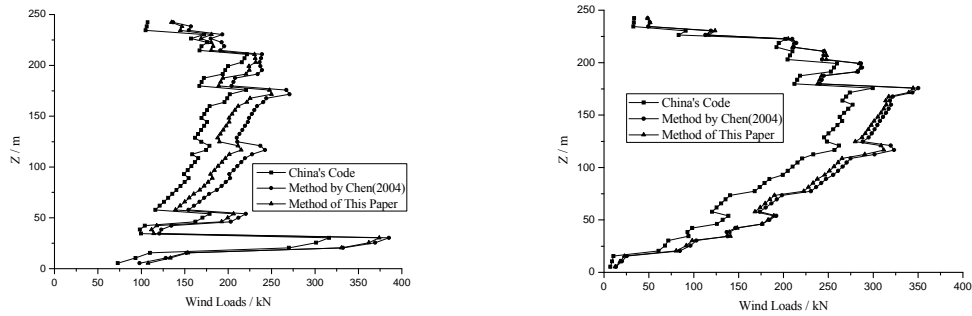
(a) Wind azimuth of  $0^\circ$ (b) Wind azimuth of  $90^\circ$ 

Fig. 15 Comparison of ESWLs in along-wind direction by different methods

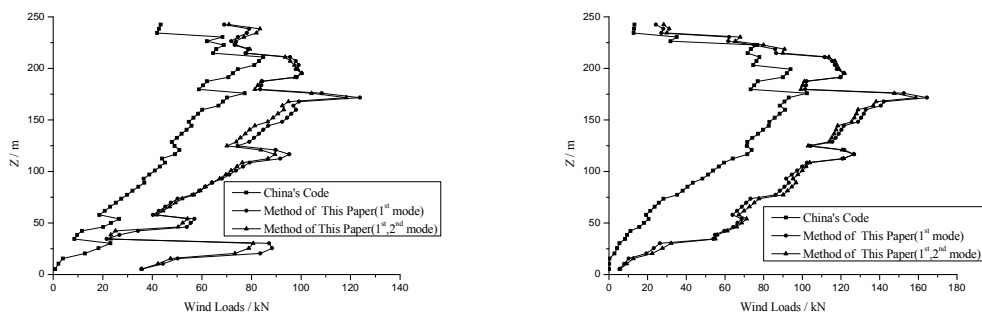
(a) Wind azimuth of  $0^\circ$ (b) Wind azimuth of  $90^\circ$ 

Fig. 16 Comparison of dynamic components of ESWLs in along-wind direction

However, in China National Standard, when the equivalent wind loads of a tall building in along-wind direction are evaluated by its formula, the interference effects induced by the surrounding buildings, the change of the mass distribution along the height of the building and the change of the along-wind force spectra along the height of the building and so on, such influence factors are not taken into consideration, and these factors can directly affect the amplitude and distribution of the equivalent wind loads in along-wind direction along the height of the tall building. The results obtained by the method proposed in this paper have taken all the above mentioned factors into account, so the distribution of the ESWLs in along-wind direction along the height of the tall building calculated by the method of this paper are more accurate.

#### 4. Conclusions

Based on the wind tunnel data, the three-dimensional ESWLs of symmetrical high-rise buildings were investigated using the mode acceleration method, and the calculation method of the three-dimensional ESWLs of symmetrical high-rise buildings based on internal force equivalence

was provided in this paper. An actual symmetrical super high-rise building was taken as an example to analyze the three-dimensional ESWLs of high-rise buildings. The main conclusions obtained in this paper are as follows:

- Based on the mode acceleration method, the wind-induced internal force response formula based on the elastic force was deduced. On the basis of the principle of internal forces equivalence, and considering the contributions of structural higher modes, the equivalent wind loads of high-rise buildings in along-wind, across-wind and torsional directions was acquired. The ESWLs obtained by the proposed method were directly based on the equivalence of each layer internal forces of a high-rise building, and were calculated according to the wind tunnel data of the building model as well as its scaled wind environment; thus they are the internal force equivalent wind loads with higher precision.
- The ESWLs of an actual symmetrical super high-rise building are calculated, and the calculated results indicate that the ESWLs of the super high-rise building in along-wind and across-wind directions are at the same order of magnitude, and its ESWLs in torsional direction also cannot be ignored. Therefore, the joint actions and combination effects of three-dimensional wind loads on super high-rise buildings should be considered in the same time for their structural wind-resistant design, as they have already been investigated by Tamura *et al.* (2014).
- For three-dimensional equivalent wind load of super high-rise structures, their quasi-static force term equivalent wind load and inertia force term equivalent wind load are at the same order of magnitude, if only adopting the inertia force term as structural equivalent wind loads will greatly underestimate the due wind loads on super high-rise structures, and accordingly, the structural design will be inclined to danger.
- The comparison is conducted between the ESWLs of an actual super high-rise building in along-wind direction calculated by the method of this paper and those obtained by China National Standard. The calculated results by the two methods are rather different, the magnitudes of the ESWLs calculated by the method of this paper are larger than those obtained by China National Standard, but the distribution tendencies of the two kinds of the equivalent wind loads along the height of the building are similar.

## **Acknowledgments**

The research presented in this paper was supported by the China National Natural Science Foundation under project No. 51178359 and 90715023, which are gratefully acknowledged, and the authors also wish to thank Dr. Eric Ho, Director of Boundary Layer Wind Tunnel Laboratory, University of Western Ontario, who carefully reviewed this paper and gave some valuable suggestions.

## **References**

- Aly, A.M. (2013a), "Pressure integration technique for predicting wind-induced response in high-rise buildings", *Alexandria Eng. J.*, **52**, 717-731.
- Aly, A.M. (2013b), "Proposed approach for determination of tributary areas for scattered pressure taps",

- Wind Struct.*, **16**(6), 617-627.
- Architecture Institute of Japan (AIJ) (1996), *Recommendations For Loads On Buildings*, Architecture Institute of Japan, Tokyo.
- Blaise, N. and Denoel, V. (2013), "Principal static wind loads", *J. Wind Eng. Ind. Aerod.*, **113**, 29-39.
- Chan, C.M., Huang, M.F. and Kwok, K.C.S. (2010), "Integrated wind load analysis and stiffness optimization of tall buildings with 3D modes", *Eng. Struct.*, **32**(5), 1252-1261.
- Chen, X. and Kareem, A. (2004), "Equivalent static wind loads on buildings: new model", *J. Struct. Eng. - ASCE*, **130**(10), 1425-1435.
- Chen, X. and Kareem, A. (2005), "Coupled dynamic analysis and equivalent static wind loads on buildings with three-dimensional modes", *J. Struct. Eng. - ASCE*, **131**(7), 1071-108.
- Davenport, A.G. (1967), "Gust loading factors", *J. Struct. Div. - ASCE*, **93**(3), 11-34.
- Davenport, A.G. (1985), "The representation of the dynamic effects of turbulent wind by equivalent static wind loads", *Proceedings of the AISC/CISC International Symp. on Structural Steel*, Chicago, 1-13.
- GB50009-2012 (2012), *Load Code for the Design of Building Structures*, China Architecture and Building Press, Beijing, China.
- Gu, M. and Zhou, X. (2009), "An approximation method for resonant response with coupling modes of structures under wind action", *J. Wind Eng. Ind. Aerod.*, **97**(11-12), 573-580.
- Holmes, J.D. (2002), "Effective static load distributions in wind engineering", *J. Wind Eng. Ind. Aerod.*, **90**(2), 91-109.
- Huang, G., Chen, X. (2007), "Wind load effects and equivalent static wind loads of tall buildings based on synchronous pressure measurements", *Eng. Struct.*, **29**(10), 2641-2653.
- Huang, M.F., Chan, C.M., Kwok, K.C.S. and Hitchcock, P.A. (2009), "Cross correlations of modal responses of tall buildings in wind-induced lateral-torsional motion", *J. Eng. Mech. - ASCE*, **135**(8), 802-812.
- Huang, M.F., Tse, K.T., Chan, C.M., Kwok, K., Hitchcock, P.A. and Lou, W.J. (2011), "Mode shape linearization and correction in coupled dynamic analysis of wind-excited tall buildings", *Struct. Des. Tall Build.*, **20**(3), 327-348.
- Islam, M.S., Ellingwood, B. and Corotis, R.B. (1992), "Wind-induced responses of structurally asymmetric high-rise buildings", *J. Struct. Eng. - ASCE*, **118**(1), 207-222.
- Kasperski, M. and Niemann, H.J. (1992), "The LRC method-a general method of estimating unfavorable wind loads distributions for linear and nonlinear structure", *J. Wind Eng. Ind. Aerod.*, **41**(1-3), 1753-1763.
- Ke, S.T., Ge, Y.J., Zhao, L. and Tamura, Y. (2012), "A new methodology for analysis of equivalent static wind loads on super-large cooling towers", *J. Wind Eng. Ind. Aerod.*, **111**, 30-39.
- Kwon, D.K. and Kareem, A. (2013), "Comparative study of major international wind codes and standards for wind effects on tall buildings", *Eng. Struct.*, **51**, 23-35.
- Liang, S., Liu, S., Zhang, L. and Gu, M. (2002), "Mathematical model of acrosswind dynamic loads on rectangular tall buildings", *J. Wind Eng. Ind. Aerod.*, **90**(12-15), 1757-1770.
- Liang, S., Li, Q.S., Liu, S., Zang, L. and Gu, M. (2004), "Torsional dynamic wind loads on rectangular tall buildings", *Eng. Struct.*, **26**(1), 129-137.
- Quan, Y. and Gu, M. (2012), "Across-wind equivalent static wind loads and responses of super-high-rise buildings", *Adv. Struct. Eng.*, **15**(12), 2145-2155.
- Rosa, L., Tomasini, G., Zasso, A., and Aly, A. M. (2012), "Wind-induced dynamics and loads in a prismatic slender building: A modal approach based on unsteady pressure measurements", *Journal J. Wind Eng. Ind. Aerod.*, **107**, 118-130.
- Solari, G. (1985), "Mathematical model to predict 3-D wind loading on buildings", *J. Eng. Mech. - ASCE*, **111**(2), 254-275.
- Spence, S.M.J., Bernardini, E. and Giofrè, M. (2011), "Influence of the wind load correlation on the estimation of the generalized forces for 3D coupled tall buildings", *J. Wind Eng. Ind. Aerod.*, **99**(6), 757-766.
- Tamura, Y., Kim, Y.C., Kikuchi, H. and Hibi, K. (2014), "Correlation and combination of wind force components and responses", *J. Wind Eng. Ind. Aerod.*, **125**, 81-93.
- Wang, D. and Liang, S. (2010), "Research on along-wind equivalent static load of High-rise Buildings", *Eng.*

- Mech.*, **27**(1), 134-140. (in Chinese)
- Zhang, X. (1988), "The current Chinese code on wind loading and comparative study of wind loading codes", *J. Wind Eng. Ind. Aerod.*, **30**, 133-142.
- Zhou, Y., Gu, M. and Xiang, H. (1999), "Along-wind equivalent static wind loads and responses of tall building: Part I: Unfavorable distributions of equivalent static wind loads", *J. Wind Eng. Ind. Aerod.*, **79**(1-2), 135-150.
- Zhou, Y., Kareem, A. and Gu, M. (2000), "Equivalent static buffeting wind loads on structures", *J. Struct. Eng. - ASCE*, **126**(8), 989-992.

CC